Synthesis of Sub-20 nm Nanoparticles of Zinc Oxide for Heat Transfer Applications

B. Kumar*,[1], M. K. Das[2], J. N. Roy[1]
[1]School of Energy Science and Engineering, Indian Institute of Technology Kharagpur - 721302, India
[2]Department of Mechanical Engineering, Indian Institute of Technology Kharagpur - 721302, India
Email: brajeshkumar998@gmail.com, manab@mech.iitkgp.ac.in, jnroy@atdc.iitkgp.ac.in,
Received 11.02.2021 received in revised form 13.12.2021, accepted 18.01.2022
doi: 10.47904/IJSKIT.12.3.2022.43-47

***Abstract*- Nanoparticle plays a vital role in heat transfer application considering this advantage, we synthesized zinc oxide nanoparticle using modified sol-gel method and characterized it using X-Ray Diffraction (XRD), Field Emission Microscopy (SEM) and High-Resolution Transmission Electron Microscopy (HRTEM). XRD and HRTEM confirm that synthesized nanoparticle is pure zinc oxide nanoparticles, with an average size of about 20 nm. Further, it is dispersed with the water to get ZnO-water nanofluid. Four samples of ZnO nanoparticles having a volume fraction of 0.01%, 0.1%, 1% and 5% are dispersed in water and sonicated for 2 hours. After sonication, thermal conductivity analysis of ZnO-water nanofluid is done by KD2 Pro. The thermal conductivity of nanofluid is compared with the base fluid. 0.01% doping shows no significant enhancement of thermal conductivity but 0.1%, 1% and 5% shows 0.5%, 4.5% and 23.7% thermal conductivity enhancement respectively. Therefore, ZnO-water nanofluid is a good thermic fluid for future heat transfer applications.**

Keywords- ZnO nanoparticle, XRD, FE-SEM, HRTEM.

1. INTRODUCTION

Different nanoparticles such as metal [1], metal-oxide [1], and polymer [2] are listed in the literature. Metal-oxide nanoparticles are most versatile due to their various characteristics and functionalities. Among different metal-oxide nanoparticles, ZnO nanoparticles are most important due to their vast area of applications, e.g., rubber industry [3] due to cross-linking property, biosynthesis [4], green synthesis of ZnO [5] etc. ZnO has 60 meV bond energy and 3.37 eV band gap energy; therefore, it is used in the electronics industry, such as electronics equipment [6]. This can also form useful stable heat transfer nanofluid prepared by sonication of nanoparticles into base fluid [7]. The available techniques for the synthesis and growth of ZnO nanoparticles using the different methods are summarized in Table 9. Reproducibility is a major issue in such techniques.

In this work, the controlled growth of ZnO nanoparticles is done by optimized precursor concentration. Multiple experiments have been carried out to optimized the controlled growth. It was very challenging to optimize the controlled growth with the high reproducibility of ZnO synthesis. This synthesis method used here is highly demanding and cost-effective, and reproducible at medium temperature range 54-66°C.

Table 9: Summary of ZnO nanoparticles synthesis.

Method	Precursors	Reaction Conditions	Particle size	References
Mechanochemical	$ZnCl_2$, Na_2CO_3, NaCl	400–800 °C	18-35 nm	[8]
Precipitation	$Zn(CH_3COO)_2$, and KOH	80–120 °C	160-500 nm	[9]
Sol-gel	$Zn(CH_3COO)_2$, $C_2H_2O_4$, C_2H_5OH	60–80 °C	~ 100 nm	[10]
	$Zn(CH_3COO)_2$, C_2H_5OH	500 °C	70 nm	[11]
Solvothermal	$Zn(CH_3COO)_2$, $Zn(NO_3)_2$, LiOH, KOH, NH_4OH	120–250 °C	100-2000 nm	[12]
Emulsion	$Zn(CH_3COO)_2$, C_7H_{16}, NH_4OH	700–1000 °C	0.05-0.15 µm	[13]

2. EXPERIMENTAL METHODS

The materials used are $Zn(CH_3COO)_2.2H_2O$, KOH, CH_3OH and C_3H_6O. ZnO nanoparticles synthesis is done by the modified methods [10-11]. In this procedure, 14.8 g of $Zn(CH_3COO)_2.2H_2O$ was dissolved in 625 ml of methanol,7.4 g of KOH in 325 ml of methanol to get their solution, respectively. The reaction has been carried out under continuous stirring of 600 rpm at 60°C for 180 min. The nanoparticles are settled at the bottom after the reaction is complete. These are collected using the centrifugation process, and excess mother fluid is removed. It is washed thrice with acetone and dried at 33°C for 6 hours. Further, it is crushed to get ZnO nanopowder. Three different samples were taken for analysis purposes to find out the reproducibility and bulk synthesis. Solution temperature, stirrer rotation and reaction time are kept distinct purposefully at 10% fluctuation, listed in Table 10.

Table 10: Synthesis parameter for different samples.

Samples	Solution temperature (℃)	Stirrer rotation (rpm)	Reaction times (min)
1	60	600	180
2	54	540	162
3	66	660	198

3 RESULTS AND DISCUSSION

Fig 5 shows ZnO nanoparticles of different samples with X-ray spectrum. All samples are prepared at different time intervals and different room temperatures. All samples show almost the same peak at the same 2θ° angle. Major peaks are appearing in Fig.1, namely (100), (002), (101), (102), (110), (103), and (112) confirm the materials synthesized are pure ZnO [JCPDS file no: 01-079-2205].

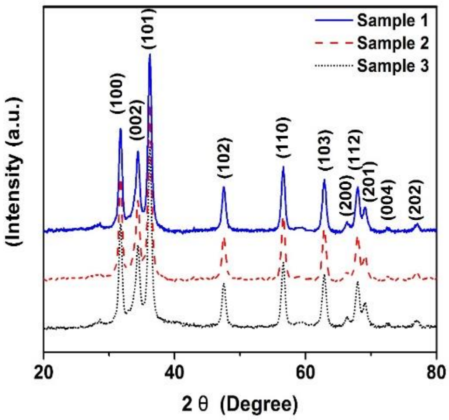

Fig 5 ZnO nanoparticles with X-ray spectroscopy of different samples.

The interplanar spacing (d) has been calculated using Bragg's law ($d = \lambda / 2\ sin\theta$) and crystal structure based on Bravais lattice parameter in which hexagonal unit cell is characterized by lattice parameter (a = 3.2496 Å) and (c = 5.2069 Å). Table 11 gives the crystallite size of ZnO nanopowders. From Table 11, it is observed that the average crystallite size of ZnO nanopowder is 17.02 nm.

Table 11: Crystallite size of ZnO nanoparticles.

No	θ(rad)	β(rad)	D (nm)
1	0.27698	0.01071	15.48
2	0.30017	0.01166	14.31
3	0.31612	0.01121	14.97
4	0.41474	0.00972	17.92
5	0.49402	0.01232	14.70
6	0.54868	0.01096	17.05
7	0.57882	0.00921	20.68
8	0.59306	0.00914	21.02

For SEM analysis, Carl ZEISS SMT, Germany, ZEISS EVO 60 Scanning Electron Microscope is used. The morphology of ZnO nanoparticles was studied by FE-SEM, which is shown in Figure 2. The FE-SEM images of ZnO nanoparticles show that they are consistent and almost spherical with about 20 nm, suitable for thermal and photocatalytic activities.

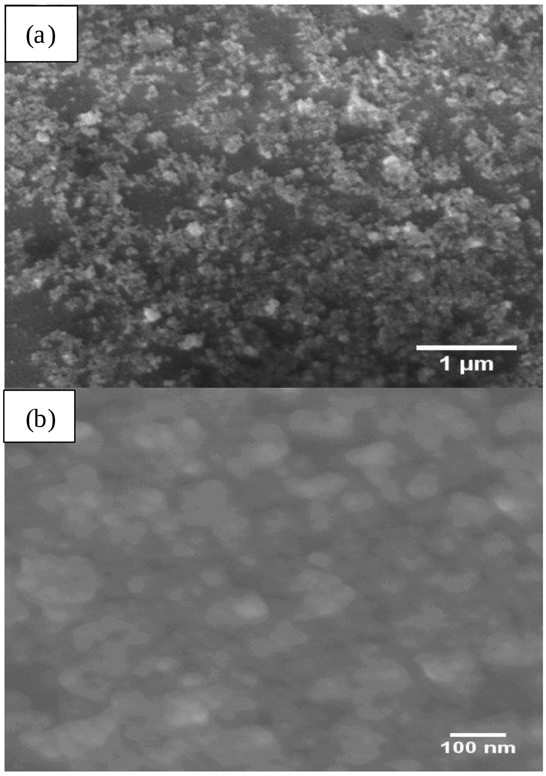

Fig. 6 SEM image of ZnO nanopowder at (a) 1 µm resolution and (b) 100 nm resolution.

HRTEM analysis has been done using JEM – 2100, JEOL, Japan, operating at Voltage 200 kV and LaB6 filament. Fig. 8 show lattice resolution images containing information on the atomic-scale structure. The inter-planar spacing (d) has been calculated using equation (1).

$$d = \frac{\lambda L}{R} \quad (1)$$

where λ (0.00251 nm) is the wavelength of the beam at 200 keV, L (400 mm) is camera length, R is the diffracted beam distance from the center. SAED pattern of ZnO nanoparticle confirms that the synthesized ZnO is Polycrystalline. Detail of the SAED pattern of ZnO nanoparticles is shown in Table 12.

Raman spectroscopy of the ZnO sample was done using Ar laser with 520 nm excitation wavelength. Figure 5 shows the Raman spectrum of ZnO. The peak at 280 cm^{-1} is the outcome of multiple scattering phonons E_2 (high) − E_2 (low). The peak at 97 cm^{-1} and 440 cm^{-1} are the characteristic non-polar mode E_2 (low) and E_2 (high) of wurtzite structure. The peaks at 403 cm^{-1} and 934 cm^{-1} are assigned to the E_1 (TO) and A_1 (2TO) modes.

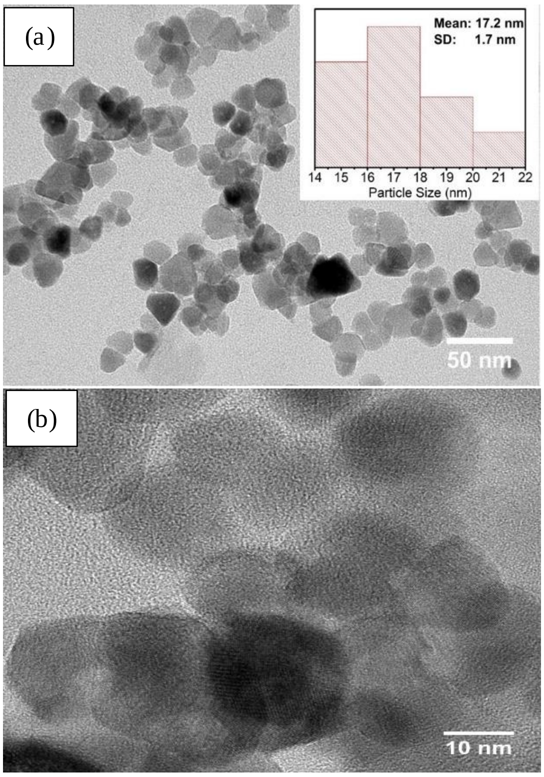

Fig. 7 HRTEM image of ZnO nanopowder at (a) 50 nm resolution and (b) 10 nm resolution.

Table 12: SAED pattern ring details of ZnO nanopowders.

Ring No.	R (1/nm)	d(nm)	hkl
1	3.475	0.28777	100
2	3.724	0.26853	002
3	3.959	0.25259	101
4	5.105	0.19589	102
5	5.99	0.16694	110
6	6.598	0.15156	103
7	6.902	0.14489	200
8	7.054	0.14176	112

ZnO.

Dynamic light scattering (DLS) analysis, using ZEN 3600 Malvern Instrument USA of ZnO nanoparticles dispersed in ethanol is shown in Fig. 10. The size was estimated to be 20.3 nm on average, with a standard deviation of 7.8 nm. The particle size of 15.5 nm and 19.6 nm have a maximum frequency of 25% and 24%, respectively. DLS particle size distribution having a perfect agreement with XRD and HRTEM results.

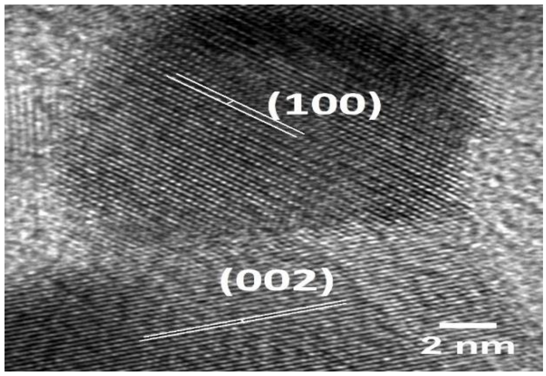

(a)

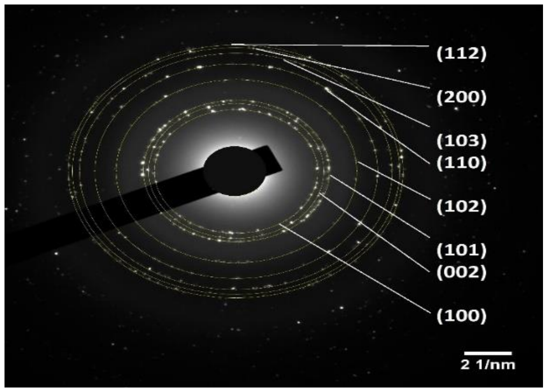

(b)

Fig. 8 HRTEM image of ZnO nanoparticles showing (a) lattice fringes and different orientation of the plane in wurtzite structure and (b) SAED pattern of nanoparticle, which shows polycrystalline of ZnO.

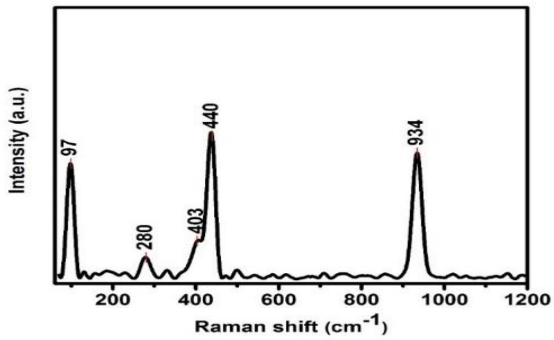

Fig. 9 Optical phonon modes in the Raman spectra of wurtzite

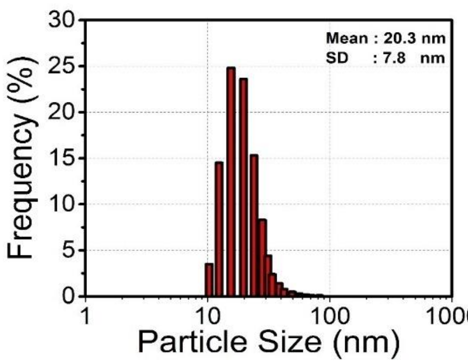

Fig. 10 The particle size distribution of ZnO nanoparticles.

For energy dispersive (EDXS) analysis, JEM-2100F (HRP) instrument has been used at the voltage of 200.0 keV and Probe current of 1 nA. Fig. 11shows the EDX spectrum of ZnO nanoparticles. Zn peaks at 0.9, 1.0, 8.6 and 9.6 keV, O peak at 0.5 keV show a strong signal of Zn and O. These results confirm the high purity of the synthesized ZnO nanoparticles. The single stare and the double star represents Cu and C peaks, respectively, which comes from the grid itself. The quantitative EDX spectra analysis of ZnO nanoparticles is shown in Table 13. For the pure ZnO nanoparticles, the mass ratios of Zinc and Oxygen signals are 85.86% and 14.14%, and the atomic ratio of Zinc and Oxygen signals is 59.75% and 40.25%, respectively.

Table 13: Quantitative analysis of EDX spectra of ZnO nanoparticles.

Element	Mass (%)	Atom (%)
Zn	85.86	59.75
O	14.14	40.25
Total	100	100

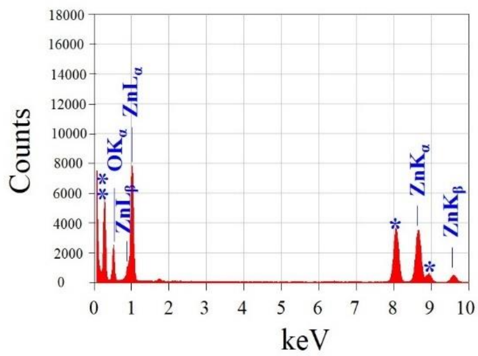

Fig. 11 EDX spectrum of ZnO nanoparticles in which electron return to K and L electron shell.

4. THERMAL CONDUCTIVITY OF NANOFLUID

Four samples of ZnO nanoparticles having a volume fraction of 0.01%, 0.1%, 1% and 5% are dispersed in water and sonicated for 2 hours with Ultrasonic Vibrator Machine (UVM) made by Schneeberger, model no. NK6-160, 3000W/20 kHz. After sonication, thermal conductivity analysis of ZnO-water nanofluid is done by KD2 Pro (ASTM Standard D5334-08 and IEEE Standard 442-1981, with ±10% thermal conductivity accuracy and 4 AA battery source). From Figure 8, it is observed that 0.01% doping shows no significant enhancement of thermal conductivity, but 0.1%, 1% and 5% shows 0.5%, 4.5% and 23.7% thermal conductivity enhancement, respectively. Therefore, ZnO-water nanofluid is a good thermic fluid for future heat transfer applications.

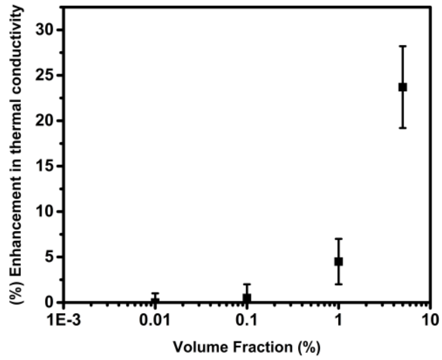

Fig. 8 Thermal conductivity measurement of different volume fractions of ZnO-water nanofluid.

5. CONCLUSIONS

The synthesis method used here is simple and reproducible for a large synthetic scale. The diffraction peaks of ZnO nanoparticle show hexagonal wurtzite crystal, which belongs to the space group of C_{6v}^{4} (P6₃mc) and 186 group number. FE-SEM image revealed the average 20 nm diameter spherical ZnO nanoparticles. HRTEM image shows that the average particle size is approximately 17.2 nm, XRD result of the average crystallite size of 17.02 nm. DLS results show an average particle size of 20.3 nm. The above results indicate the excellent dispersibility of the nanoparticles in the solvent. The Raman shift shows the wurtzite structure of ZnO nanoparticle and EDX confirm the formation of pure ZnO nanoparticles. It is observed that 0.01% doping shows no significant enhancement of thermal conductivity, but 0.1%, 1% and 5% shows 0.5%, 4.5% and 23.7% thermal conductivity enhancement, respectively. Therefore ZnO-water nanofluid is a good thermic fluid for future heat transfer applications.
Agathosma betulina is a natural extract of ZnO nanoparticle synthesis. Green synthesis of ZnO nanoparticles and its characterization for heat transfer application may be studied further.

6 ACKNOWLEDGEMENTS

The work is supported by the Indian Institute of Technology Kharagpur, India. The first author also acknowledges the Ministry of Education Academic Research Fund for Doctoral Students.

7. REFERENCES

[1] Franke M E, Koplin T J, Simon U (**2006**) Metal and Metal Oxide Nanoparticles in Chemiresistors: Does the Nanoscale Matter? *Wiley-VCH Verlag* 2:36–50.
[2] Crucho C I C, Barros M T (**2017**) Polymeric nanoparticles: A study on the preparation variables and characterization methods. *Mater Sci Eng C* 80:771–784.
[3] Mandal U K, Tripathy D K, De S K (**1996**) Dynamic mechanical spectroscopic studies on plasticization of an

ionic elastomer based on carboxylated nitrile rubber by ammonia. *Polymer (Guildf)* 37:5739–5742.

[4] Chaudhuri S K, Malodia L (**2017**) Biosynthesis of zinc oxide nanoparticles using leaf extract of Calotropis gigantea: characterization and its evaluation on tree seedling growth in nursery stage. *Appl Nanosci* 7:501–512.

[5] Meron G D, Fedlu K S, Gemechu D E and Bedasa A Ga (**2020**) Synthesis of Zinc Oxide Nanoparticles Using Leaf Extract of Lippia adoensis (Koseret) and Evaluation of Its Antibacterial Activity. J*ournal of Chemistry* 2020:1-9.

[6] Muhammad T N, Nesrine A and Michal P (**2021**) Synthesis and applications of ZnO nanostructures (ZONSs): a review. *Critical Reviews in Solid State and Materials Sciences* 2021:1-43.

[7] Lee G, Kyu C, Ku M, et al (**2012**) Thermochimica Acta Thermal conductivity enhancement of ZnO nanofluid using a one-step physical method. *Thermochim Acta* 542:24–27.

[8] Stankovic A, Veselinovic L, Skapin S D, et al (**2011**) Controlled mechanochemically assisted synthesis of ZnO nanopowders in the presence of oxalic acid. *J Mater Sci* 46:3716–3724.

[9] Jesionowski T, Krysztafkiewicz A (**2010**) Obtaining Zinc Oxide From Aqueous Solutions. Physicochem Probl Miner Process 44:93–102.

[10] Mahato T H, Prasad G K, Singh B, et al (**2009**) Nanocrystalline zinc oxide for the decontamination of sarin. *J Hazard Mater* 165:928–932.

[11] Yue S, Yan Z, Shi Y, Ran G (**2013**) Synthesis of zinc oxide nanotubes within ultrathin anodic aluminum oxide membrane by sol-gel method. *Mater Lett* 98:246–249.

[12] Dem'yanets L N, Li L E, Uvarova T G (**2006**) Zinc oxide: Hydrothermal growth of nano- and bulk crystals and their luminescent properties. *J Mater Sci* 41:1439–1444.

[13] Lu C H, Yeh C H (**1997**) Emulsion precipitation of submicron zinc oxide powder. *Mater Lett* 33:129–132.